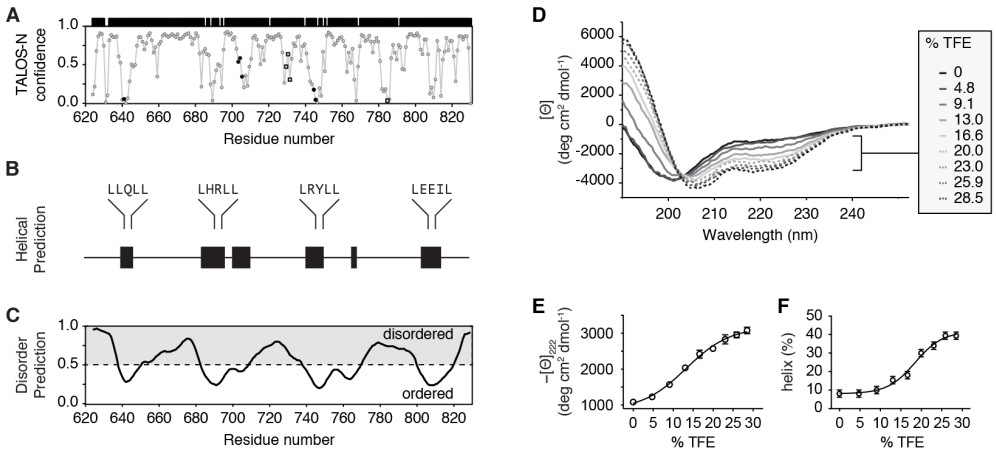

Figure S1. Related to **Figure 1**. NMR, secondary structure and disorder prediction, and CD analysis of SRC-2 RID. (**A**) TALOS-N analysis of SRC-2 RID chemical shifts, which are predictive of protein secondary structure, revealed random coil structure for most regions of SRC-2 RID except the LXXLL-containing regions, which have low confidence predictions for all secondary structure types; coil (grey circles), helix (black circles) and sheet (white squares). Black bars above depict residues with NMR assignments; white gaps indicate no NMR assignments. (**B**) Bioinformatic helical prediction by the PredictProtein web server (www.predictprotein.org) and (**C**) disorder prediction by PrDOS web server (prdos.hgc.jp) is consistent with NMR chemical shift analysis (**A**) indicating the LXXLL-containing regions have a higher probability of helical secondary structure. (**D–F**) CD spectroscopy confirms SRC-2 RID is mostly random coil with a low level of nascent helical structure; (**D**) CD spectra of SRC-2 RID with increasing concentrations of 2,2,2-trifluoroethanol (TFE), a helical secondary structure stabilizer; (**E**) CD signal at 222 nm vs. %TFE; and (**F**) K2D2-predicted helical content vs. %TFE from the K2D2 web server (cbdm-01.zdv.uni-mainz.de/~andrade/k2d2).

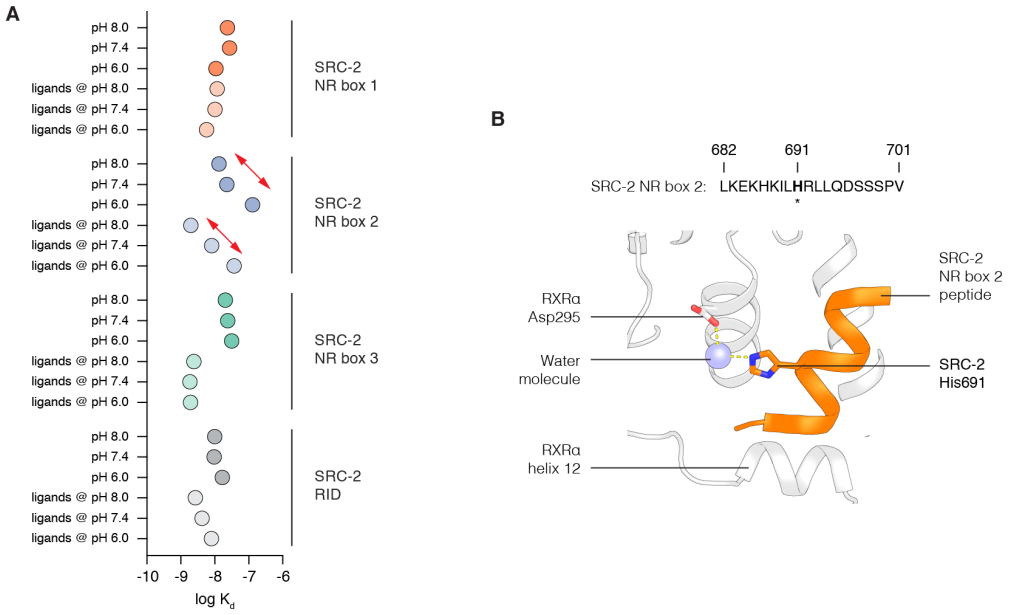

Figure S2. Related to **Figures 1 and 2**. pH dependence on the FP assay of SRC-2 RID and peptides binding to PPARγ-RXRα LBD heterodimer. (**A**) K_d values of SRC-2 RID and individual SRC-2 LXXLL peptides binding to PPARγ-RXRα LBD heterodimer ± both receptor-specific ligands (Rosi and 9cRA) determined from a FP assay performed with two experimental replicates and fit to a one-site specific binding equation. Red arrows note the large affinity change for the SRC-2 NR box 2 peptide as a function of pH relative to the other peptides and SRC-2 RID. Data collected in the presence of both ligands are shaded in lighter colors. (**B**) The SRC-2 NR box 2 peptide contains two histidine residues. In the crystal structure of DHA-bound RXRα complexed to SRC-2 NR box 2 peptide (PDB 1MV9), one of these histidine residues, His691, forms a hydrogen bond with a water molecule that is also hydrogen bonded to the sidechain of Asp295 in the RXRα AF-2 coactivation interaction surface. This indicates the protonation state of His691 could regulate the binding of SRC-2 NR box 2 peptide, which is consistent with the reduced affinity observed at acidic pH in (**A**).

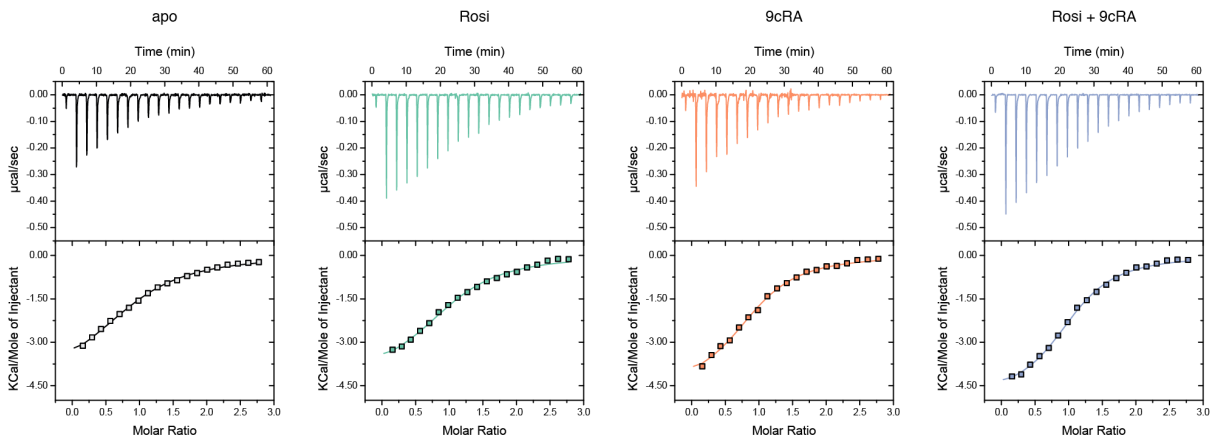

Figure S3. Related to **Figure 2**. ITC analysis of SRC-2 RID binding to apo and receptor-specific agonist bound PPARγ-RXRα LBD heterodimer.

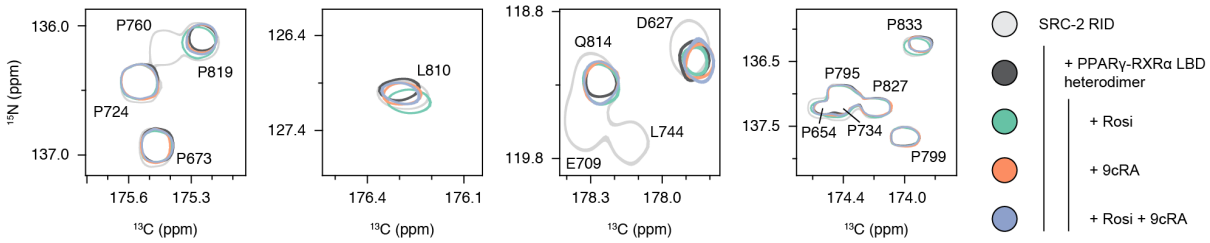

Figure S4. Related to **Figure 3**. ^{13}C-detected CON NMR of SRC-2 RID ± PPARγ-RXR*α* LBD heterodimer ± ligands. Because many NMR peaks within the LXXLL-containing regions in SRC-2 RID experienced significant line broadening and disappeared when the RID bound to PPARγ-RXR*α* (**Figure 1B-D**), this analysis was necessarily limited to regions where NMR peaks are observed, including residues in linker regions between LXXLL motifs and the C-terminal extended region. Nevertheless, when PPARγ-RXR*α* is bound to different ligands, some of the remaining NMR peaks revealed subtle chemical shift perturbations. Namely, addition of Rosi and/or 9cRA results in subtle chemical shift perturbations in linker regions of SRC-2 RID between LXXLL motifs (D627, P654, P673, P734) and the extended C-terminal region (L810, Q814, P819, P833) that does not interact with PPARγ-RXR*α*.

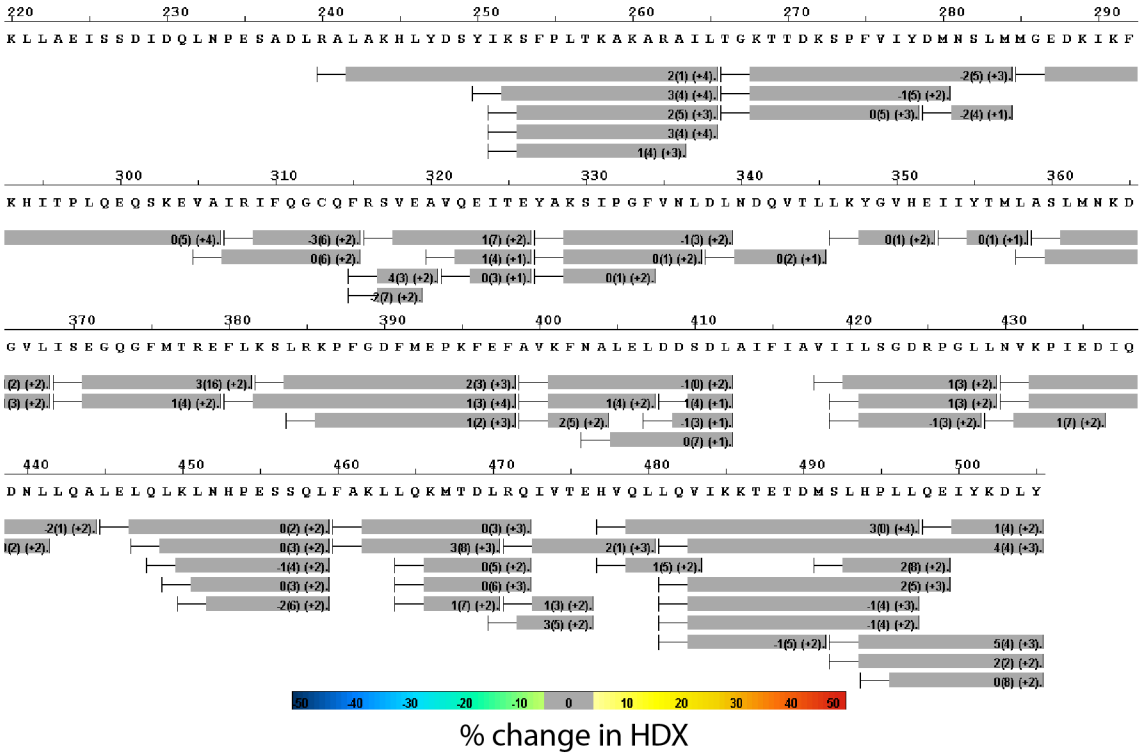

Figure S5. Related to **Figure 3**. HDX-MS analysis of delipidated vs. non-delipidated PPARγ LBD shows no significant change in solvent exchange.

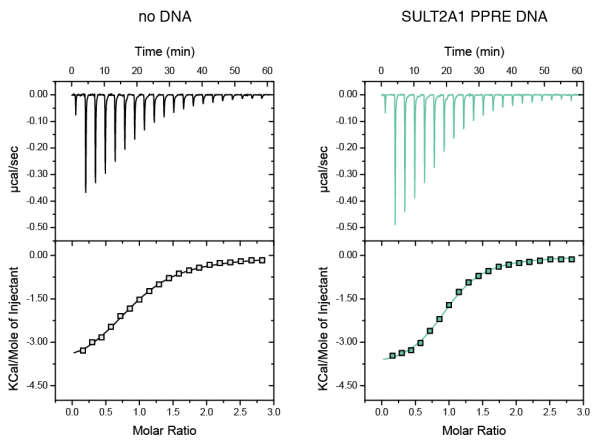

Figure S6. Related to **Figure 4**. ITC analysis of SRC-2 RID binding to full-length PPARγ-RXRα bound to receptor-specific agonists in the absence or presence of *SULT2A1* PPRE DN